W-SBA based materials as efficient catalysts for the ODS of model and real feeds: improvement of their lifetime through active phase encapsulation

G. Estephane,[a] C. Lancelot,[a,*] P. Blanchard,[a] V. Dufaud,[b] S. Chambrey,[a] N. Nuns,[c] J. Toufaily,[d] T. Hamiye,[d] C. Lamonier,[a]

[a] Université Lille, CNRS, ENSCL, Centrale Lille, Univ. Artois, UMR 8181 - UCCS - Unité de Catalyse et de Chimie du Solide, F-59000 Lille, France.

[b] Laboratoire de Chimie, Catalyse, Polymères, Procédés, CNRS, Université Claude Bernard Lyon 1, CPE Lyon, 43 Bd du 11 novembre 1918, F-69616 Villeurbanne cedex, France.

[c] Université Lille, CNRS, INRA, Centrale Lille, ENSCL, Univ. Artois, FR 2638 - IMEC - Institut Michel-Eugène Chevreul, F-59000 Lille, France.

[d] MCEMA, Lebanese University, Faculty of Science, Rafic Hariri University Campus, Hadath, Lebanon.

* Email. christine.lancelot@univ-lille1.fr; Tel. +33-3-20-43-43-87.

Abstract

Incorporated W-SBA based catalysts were prepared by a direct synthesis method involving phosphotungstic acic (HPW) together with mixed structure directing agents, and by incipient wetness impregnation for comparison purpose. In the oxidative desulfurization (ODS) of dibenzothiophene (DBT, 500 to 1500 ppmS) and of a Straight Run Gas Oil (SRGO, 2000 ppmS) in batch reactor, the impregnated solids showed higher efficiency than the incorporated ones, which was attributed to a better accessibility of the active phase present at the surface of the support in the impregnated catalysts. However, in continuous evaluation using a fixed bed reactor, the incorporated catalyst showed a stable conversion in the ODS of SRGO 2000 ppmS for 9 days while within 24h the impregnated solid was almost completely deactivated. Higher interaction of the active phase with the support in incorporated catalysts was evidenced by Time-of-Flight Secondary Ions Mass Spectrometry (ToF-SIMS) analysis, which can be at the origin of less leaching of tungsten species during reaction and thus explain their better resistance towards deactivation. The lower efficiency of incorporated catalysts compared to impregnated ones in ODS reaction carried out in a batch reactor is clearly compensated by their resistance towards leaching of the active phase in a continuous test. These results highlight the importance of evaluating not only the catalysts performance but also their lifetime in conditions more representative of industrial ones.

Keywords: oxidative desulfurization, phosphotungstic acid, incorporation, DBT, SRGO

1. Introduction

Hydrodesulfurization (HDS) is the main industrial process for the removal of undesirable sulfur containing compounds present in petroleum feedstocks. However the continuous tightening of environmental regulations concerning the sulfur content in diesel led to consider and develop complementary and/or alternative solutions, among which oxidative desulfurization (ODS) is arousing an increasing interest [1-3]. In the ODS process, the sulfur containing molecules are oxidized in sulfones, which, due to their polar properties, can be further separated from the reaction mixture by extraction or adsorption [4-6]. One major advantage of this reaction is that it is carried out under mild conditions regarding temperature and pressure and without the use of costly hydrogen [7]. Moreover, refractory

compounds in HDS such as 4,6-dimethyldibenzothiophene (4,6-DMDBT) are more readily converted in the ODS process than benzothiophene (BT), which has been related to the higher electron density on the sulfur atom in DBT than in BT [8-11].

Polyoxometalates (POM) have been extensively used as ODS catalysts in homogeneous systems, in particular Keggin-type heteropolyacids (HPA), like phospho(silico)tungstic or molybdic acids [12-15]. Due to the difficulty associated to catalyst recovery, heterogeneous systems are however preferred, with dispersion of the HPA at the surface of a carrier. Mesoporous silica have been reported as suitable supports for ODS catalysts, due to their large surface area and high stability, like HMS [16], MCM-41 [17,18] and SBA [19,20]. However these impregnated catalysts suffer from strong deactivation, which major sources have been identified as sulfones adsorption on the catalysts as well as leaching of the active phase during reaction [15,21]. It is thus of paramount importance to optimize not only the efficiency of a catalyst but also its resistance regarding deactivation. If sulfones retention on the catalyst surface is important in the ODS of model molecules, it is much less present in the ODS of real feedstocks, as sulfones are more soluble in these media [19]. Concerning the active phase leaching, several strategies aiming at the stabilization of the active phase have been developed, either by anchoring the HPA on a modified surface or through encapsulation within the silica framework by direct synthesis. For instance phosphotungstic acid (HPW) has been immobilized on the surface of MCM-41 [22,23] and SBA-15 [24] functionalized by amino groups and in all the cases the obtained catalysts could be reused without significant loss of activity in the ODS of model compounds. However modification of the support requires extra steps in the catalyst synthesis which may be detrimental to the overall cost of the process. Alternatively one-pot synthesis approaches have been developed for the incorporation of polyoxometalates, introduced during the silica support preparation [25-29]. Several authors reported on the use of such one-pot catalysts in ODS reaction [30-35] but only a few addressed the reusability of the catalytic solids. With one exception [32], the majority of the authors reported the preservation of the catalytic efficiency after several runs [33-35]. Interaction of HPW with the support was claimed to be responsible for this activity stabilization, but only Du *et al.* brought experimental evidence by FT-IR of this interaction [33].

In this work we propose to evaluate the efficiency and the lifetime in ODS of incorporated HPW catalysts with various HPW contents, prepared by a direct synthesis method in the presence of poly-(ethylene oxide)-poly(propylene oxide) copolymer (Pluronic P123) and cetyltrimethylammonium bromide (CTAB) as structure directing agents. Impregnated catalysts on SBA-15 with similar HPW contents were also prepared for comparison purpose. The originality of our work lies first in the testing of these solids, whose efficiency is not only evaluated in the ODS of model feed in batch reactor, but also in the ODS of a Straight Run Gas Oil (SRGO) 2000 ppmS using a fixed bed reactor during a 9 days period, when most of the literature deals with model feeds in batch reactors. Moreover Time-of-Flight Secondary Ions Mass Spectrometry (Tof-SIMS) analysis allowed probing the interaction between the HPW and the support depending on the preparation method.

2. Experimental methods

2.1. Materials

The main SRGO characteristics are presented in Table 1.

Sulfur concentration /ppm	10892
Monoaromatics /wt%	16.7
Diaromatics /wt%	10.4
Triaromatics /wt%	1.2
Total nitrogen concentration /ppm	162
Density at 15°C /g.mL^{-1}	0.85
Boiling T° range /°C	181-362
Cetane Index	54.96
BT /ppm	32
Cx-BTs /ppm	4718
DBT /ppm	249
Cx-DBTs /ppm	5393

Table 1: Main characteristics of SRGO.

Phosphotungstic acid (HPW, 99.995%), cetyltrimethylammonium bromide (CTAB, 99%), P123 (30% PEG), dodecane (99%), tert-butyl hydroperoxide (TBHP, 5.0-6.0 M in decane), chlorhydric acid (HCl,

11.3 mol.L^{-1}), dibenzothiophene (DBT, 98%) were purchased from Sigma-Aldrich and tetraethyl orthosilicate (TEOS, 99%) from Fluka.

2.2. Support and catalysts synthesis

SBA preparation:

The SBA-15 support was prepared under classical acidic conditions [36]. Triblock copolymer P123 ($EO_{20}PO_{70}EO_{20}$, 12.0 g) was dissolved in water (370 g) acidified with HCl (37 g). The solution was then heated at 40 °C. After the complete dissolution of the copolymer, tetraethyl orthosilicate (24 g) was slowly added under vigorous stirring to give a gel with a TEOS/P123/HCl/H_2O molar ratio of 1:0.018:3.3:187. The transparent solution was stirred at 40 °C for 24 h. The obtained milky solution was then transferred to a Teflon lined autoclave and heated at 100 °C for 24 h. After cooling down the autoclave to room temperature, the white solid collected by filtration was washed with distilled water before drying at 80 °C overnight. Before characterization and subsequent use, the solid was calcined under air at 500 °C for 8 h (1 °C.min^{-1}).

Impregnated catalysts:

W-based catalysts were prepared by incipient wetness impregnation of a solution of phosphotungstic acid $H_3PW_{12}O_{40}$ on the SBA support with HPW contents between 6 and 25 wt%. After impregnation and maturation for 3 h, the obtained solids were dried overnight in an oven at 75 °C before calcination under air flow at 500 °C for 8 h with a temperature increase rate of 1 °C.min^{-1}.

Direct synthesis:

Incorporated catalysts were prepared by a direct synthesis method based on the protocol elaborated by Dufaud *et al.* for the incorporation of HPA in SBA-15 support, involving the polymerization of a silica precursor in the presence of the heteropolyacid and using a mixture of non-ionic (Pluronic123) and ionic (cetyltrimethylammonium bromide, CTAB) structure directing agents [37]. Mixed micelles with ionic surfactants allowed a change in surface charge distribution at the surface of the micelle, leading to stronger interactions between the template, inorganic precursor and included polyoxometalates. In a typical synthesis, 32.6 g of TEOS, 16 g of P123 and 0.8 g CTAB were combined in 500 mL of HCl solution (1.9 M) and allowed to react at 40 °C for 45 minutes (prehydrolysis step). Phosphotungstic acid,

solubilized in a minimum of acidic water, was then added dropwise, the introduced quantity being imposed by the required tungsten content in the calcined catalyst (between 5 and 19 wt% HPW). The temperature was maintained at 40 °C for 20 hours followed by ageing during 24 hours at 100 °C. The solid was recovered by filtration, washed with water and dried at 70 °C. The templates were removed by calcination at 225 °C for 6 h and then 500 °C for 20 h with a ramp of 1 °C.min^{-1}.

The prepared catalysts were named xW/SBA when prepared by impregnation and xWSBA when obtained by direct synthesis, x being the HPW content in wt%.

2.3. Material characterization

Powder X-ray diffraction (XRD) patterns were recorded on a SIEMENS D5000 diffractometer equipped with a CuKα anticathode (λ = 1.5406 Å), for 2θ between 10° and 80°, using a 0.1° step with an integration time of 4 s. Phase identification was carried out by comparison with the JCPDS database. Low-angle XRD measurements were recorded using a Bruker AXS D5005 diffractometer with CuKα radiation as an X-ray source in the range of $0.75° \leq 2\theta \leq 5°$ with steps of 0.01 °/10 s.

N_2 adsorption-desorption isotherms were recorded at -196 °C using an automated ASAP2010 instrument from MICROMERITICS. A known mass of sample (around 0.200 g) was heated at 350 °C under vacuum for 3 h. Specific surface areas (SSA) were calculated from the linear part of the Brunauer-Emmett-Teller curve. Pore size distributions were obtained by applying the Barrett-Joyner-Halenda (B.J.H.) equation to the desorption branch of the isotherm and total pore volume was estimated from the N_2 uptake value at $P/P_0 = 0.98$.

W species present on the support were identified by Raman spectroscopy. Spectra of the oxidic precursors were recorded at room temperature, using a Raman microprobe Infinity instrument from Jobin-Yvon, equipped with a N_2 cooled CCD detector. The exciting laser source was the 532 nm line of a Nd-YAG laser.

W content of the catalysts after calcination has been confirmed by X-ray fluorescence on a Bruker M4 Tornado.

Time-of-Flight Secondary Ion Mass Spectrometry (ToF-SIMS) measurements were performed with a TOF.SIMS 5 spectrometer (ION-TOF GmbH Germany) equipped with a bismuth liquid metal ion gun

(LMIG). The compacted samples were bombarded with pulsed Bi_3^+ primary ion beam (25 keV, 0.25 pA) rastered over a 500 × 500 μm^2 surface area. With 25 scans and 128x128 pixels, the total primary ion dose does not amount up to 10^{12} ions/cm^2 ensuring static conditions. Charge effects due to primary ion beam were compensated by means of a 20 eV pulsed electron flood gun. Cycle time was fixed at 220 µs in order to detect secondary molecular ions up to 4000 m/z. The mass resolution (m/Δm) measured on our spectra was about 6000 at m/z = 232 for WO_3^-. This excellent mass resolution allowed us to identify high m/z ionic fragments by their exact mass and attribution was always confirmed by the simulated isotopic pattern. In order to verify the homogeneity of the solids, 2 zones were analysed on each of the studied samples.

2.4. Catalytic evaluation in ODS reaction

2.4.1. ODS catalytic test

Catalysts performance were evaluated in the ODS of dibenzothiophene and of a SRGO with 2000 ppmS, in batch and fixed bed reactor.

Test in batch reactor: The oxidation reaction was performed in a 200 mL batch reactor under reflux. The solution to be desulfurized was first loaded in the reactor and heated to 75 °C. Catalyst and oxidant (TBHP) were added simultaneously to the reaction mixture under stirring at 700 rpm, the ratios mass(catalyst)/mass(solution) being set at 0.01 and 0.02 and the O/S ratio at 2.3 and 25 for model and real charges, respectively. Indeed, O/S ratios only slightly higher than the stoichiometric one (equal to 2) are required in the ODS of model fuels [1,2,21] while much larger values (above 15) are reported in the literature when real feeds are treated [4,38]. These high values are justified by possible secondary oxidation reactions of aromatics or nitrogen compounds present in these feeds. At the end of the test, the catalyst was recovered by filtration and washed with methanol to extract the sulfones retained on the catalyst surface.

Test in continuous fixed-bed reactor: The reactor consists of a double jacketed glass tube with a length of L = 78.5 cm and an internal diameter Ø = 5 mm. The temperature of the reactor (75 °C) is kept constant by circulating water at 75 °C in the double jacket of the reactor. The temperature profile of the

reactor has shown that an isothermal zone of 50 cm is obtained at the center of the reactor. The catalyst powder was milled and sieved to obtain particles with a diameter of 0.3 mm to prevent preferential paths. Textural analyses were performed for the catalysts after sieving showing that the textural properties were unchanged. 6 mL of catalyst was loaded at the center of the reactor (which corresponds to a catalyst bed of 30 cm inside the isothermal zone). On either side of the catalyst two beds (4.7 cm^3 for each of them) of 0.25 mm silicon carbide (SiC) were introduced to fill the reactor. It has been verified that the catalyst does not migrate through the SiC during the catalytic test. The feed direction was from bottom to top in order to avoid preferential paths of the liquid. The initial charge to be desulfurized, mixed with TBHP, was fed into the reactor by an HPLC pump with a flow rate of 0.1 $mL.min^{-1}$. The tests were carried out at atmospheric pressure and a reaction temperature of 75 °C, with a O/S molar ratio = 25 and a hourly space velocity of 1 h^{-1} corresponding to the ratio of the flow rate of the charge to the volume of catalyst. Samples were taken at regular intervals as the reaction proceeded to be analyzed.

2.4.2. Analysis of reaction products

Reaction medium and washing solutions were analyzed by UV fluorescence on an Antek 9000 apparatus to determine the total sulfur content and by gas phase chromatography on a Varian 3800 equipped with a sulfur specific detector Sievers SCD 355 (GC-SCD) to identify and evaluate the quantity of sulfur containing compounds. These analyses allowed calculating the conversion of the sulfides and the retention rate of sulfones. The retention rate is calculated as the difference of the sulfur content in the initial solution and in the reaction solution after filtration and corresponds to sulfones precipitated and/or retained on the catalyst. Analysis of the washing solutions by chromatography confirmed the exclusive presence of sulfones. Sulfur balances were found in all cases close to 100%.

In model solutions, the conversion of sulfides was obtained by dividing the mass of sulfur in the formed sulfones by the initial mass of sulfur in the sulfur compounds (formula 1). The mass of sulfones is deduced from the quantity of sulfones present in the reaction mixture and in the washing solutions of the catalyst (formula 2, 2', 2") and is calculated considering the global amount of sulfur in the solutions as determined by UV fluorescence and the relative intensities of the chromatogram peaks of sulfides and sulfones present in these solutions (formula 3). For these calculations we have considered that the

response factors of the different sulfur containing molecules (sulfides and sulfones, with alkyls groups or not) are similar since each type of molecule contains only one sulfur atom.

$Conv = mass(sulfones)/mass(S_{tot})$ (1)

$mass(sulfones) = mass(sulfones)_{reac} + mass(sulfones)_{wash}$ (2)

$mass(sulfones)_{reac}$ = mass(sulfones) in the reaction medium (2')

$mass(sulfones)_{wash}$ = mass(sulfones) in the washing solution (2")

$mass(sulfones)\ in\ i\ solution = (A_{sulfones} / (A_{sulfides}+A_{sulfones})) \times S_{tot}$, i= reac or wash (3)

A_j being the area of the compound j in the chromatograms

S_{tot} being the total sulfur content of the solution as determined by UV fluorescence

In SRGO, considering the complexity of the chromatograms of the feed and of the reaction medium, only conversion of a family of compounds (alkyl-benzothiophenes noted Cx-BT) could be monitored by integration of the corresponding peaks in the chromatograms.

3. Results and discussion

3.1. Catalysts characterization

3.1.1. Physical properties of the catalysts

On the small angle XRD patterns of the calcined bare SBA-15 and catalysts (Figures 1a and 1b), one clearly observes the three characteristic peaks of SBA-15 corresponding to the (100), (110) and (200) lattice plan of its hexagonally ordered mesophase [39]. For all the catalysts, the three peaks were maintained, indicating the preservation of the mesoporous structure of the SBA support upon impregnation as well as incorporation. Decrease in intensity of the peaks when the W content increased can be attributed to X-ray absorption by tungsten atoms [40]. Preservation of the hexagonal structure of SBA-15 upon encapsulation of POM by the same protocol used herein was also observed by Silva *et al.* and verified by TEM analysis [41].

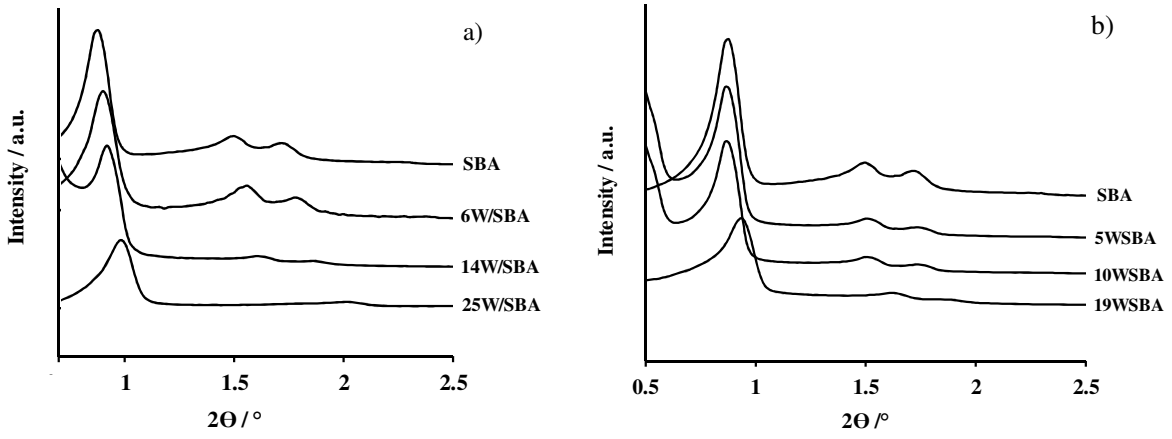

Figure 1: Low angle X-rays diffractograms of a) impregnated xW/SBA and b) incorporated xWSBA catalysts.

The nitrogen adsorption-desorption isotherms obtained for the silica support and for the HPW derived catalysts (Figures 2a and 2b) correspond to type IV according to the IUPAC classification, indicating the preservation of the mesoporous network of the SBA-15 upon impregnation and incorporation processes.

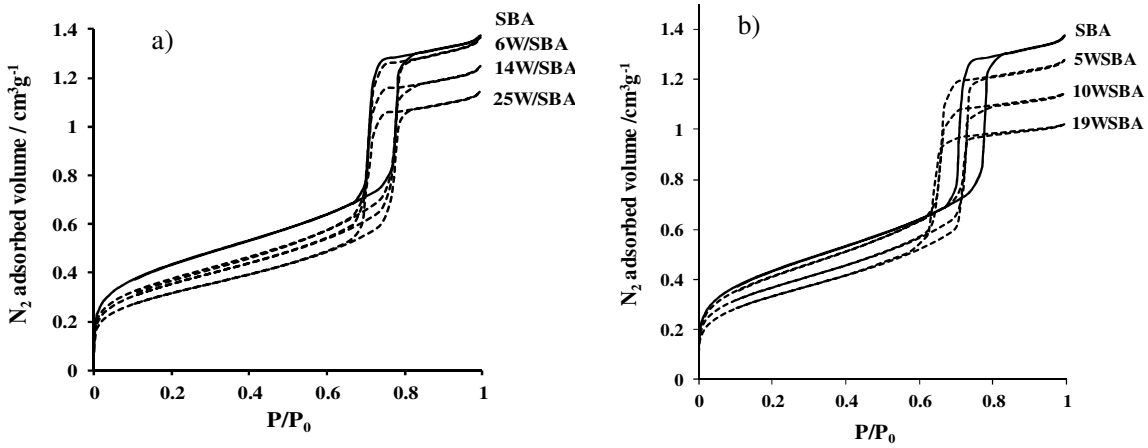

Figure 2: N_2-physisorption isotherms of a) impregnated xW/SBA and b) incorporated catalysts xWSBA.

Table 1 shows the comparison of the textural parameters of the support and catalysts. To enable direct comparison with the support, specific surface area and pore volume of the catalysts were corrected taking into account the contribution of the weight gain consecutive to the introduction of the active phase. For both series of solids, surface area and pore volume of the support were not noticeably

impacted upon impregnation and incorporation processes. While the pore diameter remained almost constant for the impregnated catalysts with respect to bare SBA-15, a slightly lower value of 6.0 nm is noticed for the incorporated catalysts, this value remaining unchanged when increasing the HPW content.

Sample	S_{BET} / m^2g^{-1}	V_p / cm^3g^{-1}	D_p / nm
SBA	1002	1.4	7.4
6W/SBA	863[a]/917[b]	1.4 [a]/1.5[b]	7.3
14W/SBA	819 [a]/952[b]	1.3 [a]/1.5[b]	7.2
25W/SBA	729 [a]/972[b]	1.2 [a]/1.6[b]	7.3
5WSBA	954[a]/1004[b]	1.3 [a]/1.4[b]	6.0
10WSBA	845[a]/939[b]	1.2 [a]/1.3[b]	6.0
19WSBA	770[a]/950[b]	1.2 [a]/1.5[b]	5.7

[a] in m^2/g of catalyst , [b] in m^2/g of silica

Table 2: Textural properties of xW/SBA and xWSBA catalysts.

3.1.2. Identification and dispersion of the tungsten species within the catalysts

Raman spectroscopy analysis was performed on the incorporated solids after calcination (Figure 3).

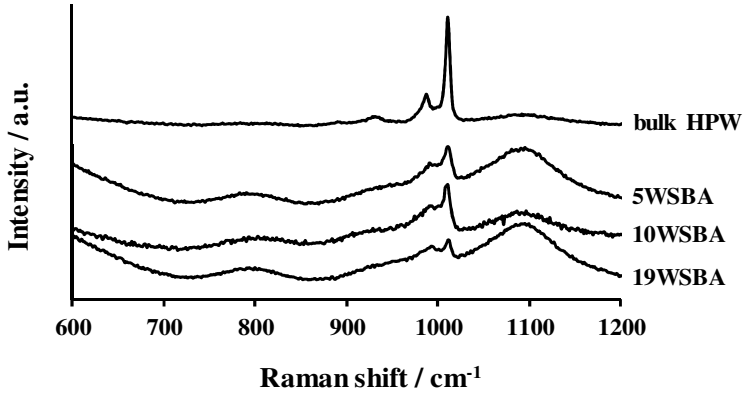

Figure 3: Raman spectra of bulk HPW and calcined incorporated catalysts xWSBA.

The broad lines pointed at 780 and 1090 cm^{-1} correspond to Si-O vibration modes of the SBA support. For all catalysts, the characteristic lines of HPW have been identified at 1009, 992 and 930 cm^{-1} [42] indicating the presence of intact HPW clusters after calcination. The presence of HPW after calcination

at 400 °C has already been evidenced on the impregnated catalysts xW/SBA by Raman spectroscopy [19] and on one-pot HPW-HMS solids by FT-IR [30].

The high angle XRD patterns (not shown here) for calcined catalysts in the 2θ range between 10 and 80° showed only a broad peak around 24° corresponding to the amorphous silica pattern. The absence of peaks characteristic of tungsten crystallized species indicated that tungsten is present in well-dispersed phase at the surface of the SBA support for both impregnated and incorporated solids. The HPW density in 25W/SBA impregnated catalyst, which is the solid with the highest W loading, is 0.07 HPW per nm^2. The size of HPW being no more than 1 nm^2, this density allows the HPW to exist as dispersed entities. Moreover the absence of bulk HPW has been reported at much higher densities, up to 0.28 $HPW.nm^{-2}$ in HPW supported on silica TUD-1 [45]. Gagea *et al.* detected the presence of bulk HPA from a density of 0.14 HPW per nm^2 of SBA [26] and Dong *et al.* from a density of 0.21 HPW per nm^2 of SBA [43], depending on the preparation method.

3.1.3. Interaction between HPW and the SBA support

All impregnated catalysts and one incorporated solid, 19WSBA, were analyzed by ToF-SIMS, in order to compare the interaction between HPW and silica depending on the preparation method. Among the advantages of using ToF-SIMS for the analysis of catalysts is first its ability to probe the top layers of the surface (1-3 nm) which is crucial in the field of catalysis. This is a clear advantage compared to other spectroscopic techniques such as XPS which provide analysis up to 10 nm in depth. The high sensitivity of ToF-SIMS (in the range of ppm-ppb) constitutes also an advantage comparing to XPS for which sensitivity is around 100 ppm. Finally, the most important specificity of ToF-SIMS in the scope of this study is the ability to provide both atomic and molecular ions giving direct information on the support-supported species interaction. Fragments recorded on pure SBA ($Si_xH_yO_z^-$) and on bulk HPW (PO_z^- ,$W_xO_z^-$, $PW_xO_z^-$) are listed in Supplementary Information. For all the catalysts, in addition to $Si_xH_yO_z^-$ and $P_xW_yO_z^-$ fragments associated to the support and HPW, a new fragment was noted, as illustrated in Figure 4 on 19WSBA catalyst. According to the exact mass and also to the relative intensity of the seven most intense peaks of this new fragment, it was possible to assign this pattern to $Si_2WO_8H^-$. Indeed, a simulation of the isotopic pattern (Figure 4) taking into account the natural abundance of the five

tungsten isotopes and the three silicon isotopes confirmed unambiguously the proposed structure. The presence of this fragment indicated a close interaction between HPW and the SBA support, both in the impregnated catalysts and the incorporated one.

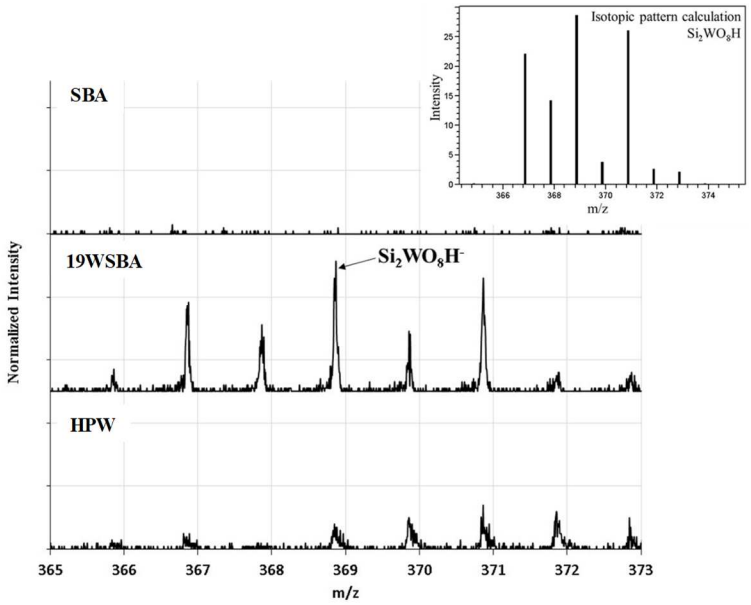

Figure 4: Identification of $Si_2WO_8H^-$ fragment on 19WSBA catalyst and simulation of its isotopic pattern.

A quantitative study of the different fragments was carried out based on the area of the peak corresponding to the major isotope. The number of counts associated to a peak was divided by the sum of the number of counts associated to all the peaks identified above. Relative areas associated to all $Si_xHO_y^-$ fragments were similar on all samples, regardless of the HPW content (Figure SI1). Indeed, the number of fragments related solely to the support is very high compared to other fragments and is thus not affected by the presence of HPA, regardless of content.

Figure 5 presents the areas associated to fragments $W_xO_y^-$, $PW_xO_y^-$ and $Si_2WO_8H^-$ related to the supported phase divided by the area of $Si_xHO_y^-$ fragments related to the support. For all the catalysts except the impregnated one with a high content 25W/SBA, the ratios associated to fragments $W_xO_y^-$ and $PW_xO_y^-$ were similar for the two analyzed zones, indicating good sample homogeneity. In the case of the high loaded 25W/SBA impregnated solid, the observed heterogeneity could stem from the formation of aggregates on some parts of the support. On the impregnated solids having a HPW loading comprised between 6 to 14%, an increase in the interaction of tungsten entities with the support was noted (more

$Si_2WO_8H^-$ fragments), in agreement with the good dispersion of the HPW entities throughout the silica surface observed for those solids. The solid with 25% HPW showed a strong increase in the number of detected $W_xO_y^-$ and $PW_xO_y^-$ fragments while the area of $Si_2WO_8H^-$ fragments remained close to that of 14W/SBA despite a higher W content. It seems that for this solid, the interaction between the tungsten species and the support is weaker, in relation with the formation of agglomerates of HPW which can thus release more $W_xO_y^-$ and $PW_xO_y^-$ fragments. To our knowledge, only two papers reported Tof-SIMS investigation of supported materials also evidencing the presence of fragments arising from both the support and the supported phase, in Mn/hydroxyapatite [44] and in Pd/$LaMnO_3$ [45] solids prepared by wet impregnation.

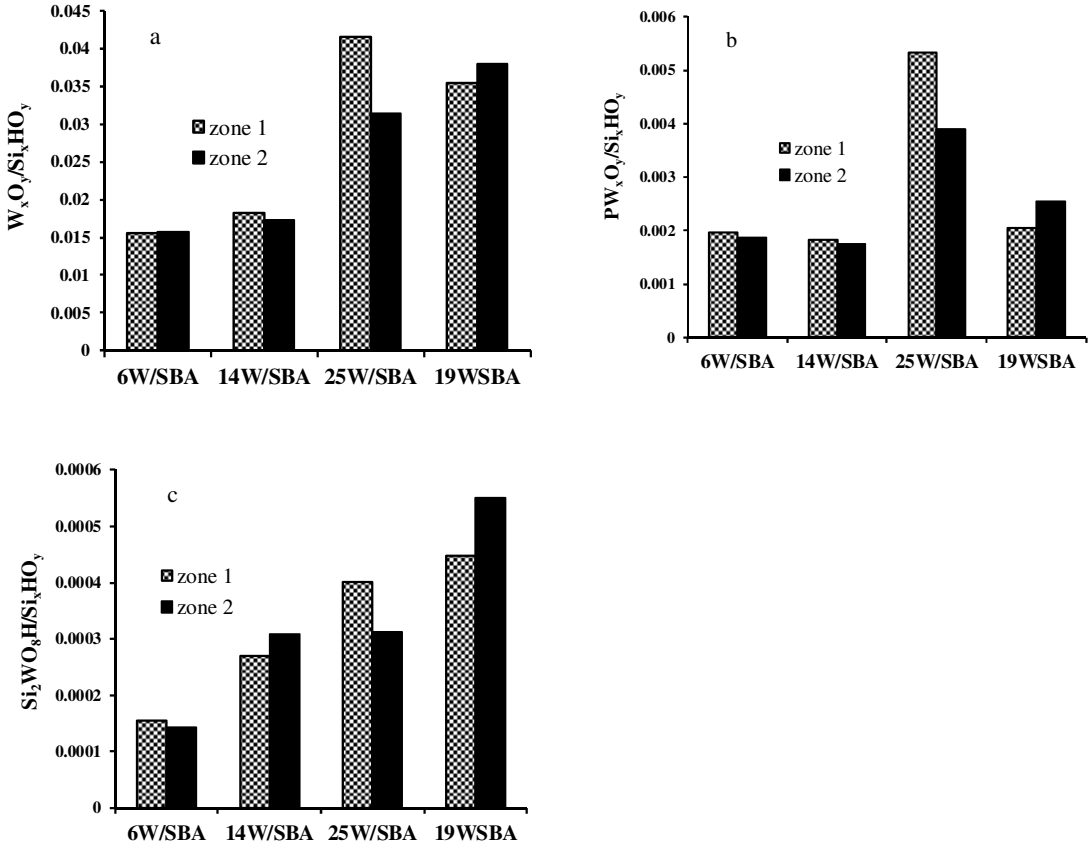

Figure 5: Fragments contribution on xW/SBA and 19WSBA: a) $W_xO_y^-$, b) $PW_xO_y^-$, c) $Si_2WO_8H^-$.

In the case of the incorporated catalyst 19WSBA, the amount of recorded fragments $W_xO_y^-$ is close to that of the impregnated solid 25W/SBA, while the $PW_xO_y^-$ fragments are less numerous. A significant increase in the intensity of $Si_2WO_8H^-$ fragment is also observed. The one-pot synthesis clearly allows enhancing the interaction between tungsten phase and silica, compared to the impregnation method.

3.2. Oxidative desulfurization properties of the catalysts

3.2.1. ODS of a model solution of DBT in batch reactor

ODS experiments were performed on a solution of DBT in dodecane with 500 ppmS with addition of 500 ppmS after one and two hours of reaction (keeping the same O/S ratio). Table 2 shows the conversions after one hour of reaction (on 500 ppmS DBT), one hour after the first addition of 500 ppmS (globally on 1000 ppmS DBT) and one hour after the second addition (globally on 1500 ppmS).

After one hour of oxidation, impregnated and incorporated solids showed similar behaviors with 100% of DBT converted. After further additions, the impregnated catalysts underwent a small decrease in performance. The conversions were however maintained between 95 and 98% one hour after the first addition and between 91 and 98% one hour after the second one, the lowest values being obtained on the 6W/SBA catalyst. In comparison, the incorporated solids exhibited lower performance than their impregnated analogues, especially noticeable one hour after the second addition, with conversions between 66 and 88%. Again, the less efficient catalyst was that with the lowest W content: 84% of conversion was obtained on 10WSBA against only 66% on 5WSBA. At the end of the experiment, between 88 and 96% of the formed sulfones were retained on the impregnated solids, with slightly lower values on the xWSBA catalysts, between 68 and 88%. One possible explanation to account for these results is that in the xWSBA solids, at a given loading, HPW entities are not equally accessible to the DBT molecules, depending on their degree of incorporation. When the sulfur content increases in the reaction medium, less tungsten atoms are proportionally available to the molecules to be oxidized, thus explaining the better performance of impregnated catalysts where all the active phase is accessible on the surface of the carrier. This is particularly significant at low HPW loading, explaining the lower efficiency of the 5WSBA catalyst. Similar conclusions were drawn by Yang *et al.* when comparing the behavior of impregnated and incorporated HPW-SBA catalysts in esterification reaction [46].

Compared to other catalytic systems, our HPW catalysts, whether impregnated or incorporated, showed greater performance in the ODS of DBT 500 ppm. For instance, Xie *et al.* observed on a W based catalyst supported on functionalized MCM-41 a conversion of DBT of 95% after one hour of reaction. However, when increasing the sulfur content to 800 ppm of DBT, a marked decrease in conversion to 78% was

shown [23] which is far below the values obtained with our impregnated (95-98%) and incorporated (83-95%) catalysts at 1000 ppmS of DBT (Table 3). Using HPW-TUD-1 catalysts prepared by direct sol-gel synthesis, Tang *et al.* obtained a DBT (500 ppm) conversion of 40% for the catalyst with 10% WO_3 and around 80% for the solids with 19 and 29% WO_3 (after one hour of test and with O/S = 8), while a total conversion of DBT was obtained after one hour of test with a lower O/S ratio on our solids regardless of the method of preparation [25]. Long *et al.* also used a tungsten based catalyst where ammonium tungstate was impregnated on a resin (D152). ODS of DBT 400 ppm was performed with cyclohexane peroxide (CHPO) as oxidant (O/S = 2.5) followed by extraction with N,N-dimethylformamide. The overall sulfur removal was measured at 99.1%, however the value without catalyst, with only extraction, was already of 86.5% [47].

Catalysts	6W/SBA	14W/SBA	25W/SBA	5WSBA	10WSBA	19WSBA
Conv (1)/% 500 ppmS	100	100	100	100	100	100
Conv (2)/% 1000 ppmS	95	97	98	83	95	92
Conv (3)/% 1500ppmS	91	98	97	66	84	88
Retention/%	88	96	96	68	69	88

Table 3: conversions of DBT on xW/SBA and xWSBA and retention rates of sulfones on the catalysts at the end of the experiment (batch reactor, 75 °C, O/S = 2.3, addition of 500 ppmS after 1 and 2 h of reaction).

3.2.2. Oxidation of a SRGO in batch reactor

The catalysts were then tested in the oxidation of a Straight Run Gas Oil containing 2000 ppm of sulfur (SRGO2000) and obtained by dilution of a SRGO containing 1% sulfur with a Light Gas Oil (LGO) with 50 ppmS. In the litterature, ODS of SRGO and diesel fraction with high sulfur content has been reported but is often associated with extraction thus giving a global sulfur removal : values around 60% of sulfur removal have been measured in the ODS of a SRGO with 16370 ppmS [48] and of a diesel

fraction with 2050 ppmS [49]. In our case, GC-SCD allowed us to follow the evolution of the sulfide species in the reaction medium. Our feed contains alkyl benzothiophenes Cx-BTs (retention times below 16 min) and alkyl dibenzothiophenes Cx-DBTs (retention times higher than 16 min) (Figure 6). On 6W/SBA, low intensity sulfones peaks began to appear at 5 min of reaction and increased up to 35 min, while BTs peaks decreased slowly and have almost disappeared at 1h of reaction. 14W/SBA and 25W/SBA appeared more efficient, sulfones being present in large quantity at 5 min and Cx-BTs being almost totally converted at 16 min (Figure SI2) [19]. In the incorporated solids, decrease of the sulfur peaks was more gradual when increasing reaction time and HPW content, with however all Cx-BTs converted at 1h (Figure 6). The quantity of retained sulfones on the catalyst was calculated on 14W/SBA and 19WSBA solids after one hour of test and corresponded to 19% and 14% of the formed sulfones respectively. These values are much lower than those measured in the ODS of DBT, sulfones being more soluble in real feeds like LGO and SRGO as reported by Estephane *et al.* [19].

On the chromatograms after oxidation, sulfones derived from Cx-BTs appeared in the zone of the Cx-DBTs. However, in the range of retention times prior to 16 min, the quantity of the Cx-BTs can be monitored without interaction with other compounds. Their conversion, presented in percentage in Figure 7, was very similar on catalysts 14W/SBA and 25W/SBA and appeared to be slower on 6W/SBA, even though at 1h of reaction all solids presented almost the same efficiency. 50% of Cx-BTs were converted in 18 min on 6W/SBA and in about 5 min on 14W/SBA and 25W/SBA, while all Cx-BTs were converted in 35 min and 17 min on 14W/SBA and 25W/SBA respectively. All incorporated solids were less active than their impregnated counterparts and improvement of their efficiency with increased HPW content was more gradual: 50% of the Cx-BTs was converted in 35 min, 23 min and 9 min on 5WSBA, 10WSBA and 19WSBA respectively. This behavior is in agreement with that observed in the ODS of DBT, in relation with more accessible active phase in the case of impregnated solids.

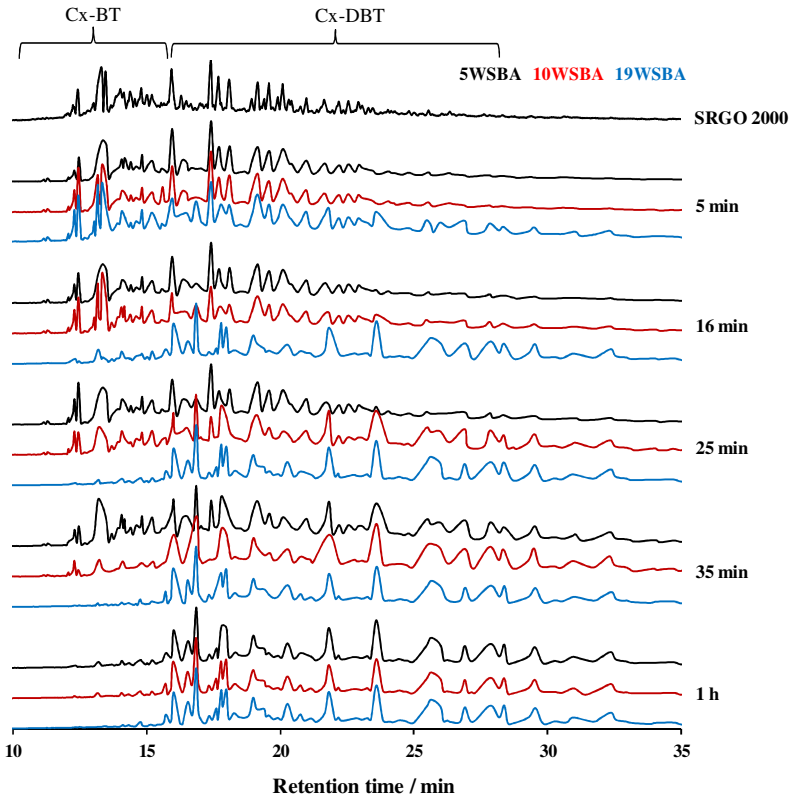

Figure 6: Chromatograms of the reaction mixture in the ODS of SGRO2000 on xWSBA, with x = 5, 10, 19 (batch reactor, 75 °C, O/S = 25).

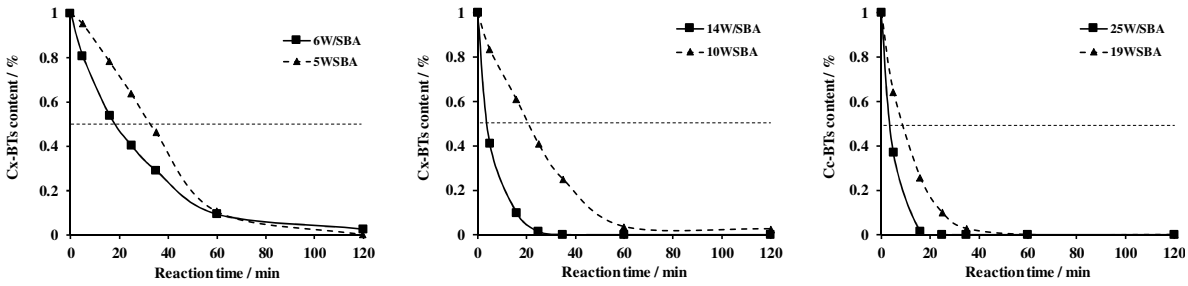

Figure 7: Evolution of Cx-BTs in the ODS of SGRO2000 for xW/SBA and xWSBA catalysts (batch reactor, 75 °C, O/S = 25).

3.2.3. ODS of SRGO2000 in a fixed bed reactor

The most efficient solids in the ODS of model and real SRGO feed in batch reactor, 25W/SBA and 19WSBA catalysts, were selected for testing in a continuous ODS test of SRGO2000 using a fixed-bed reactor. Collection of samples was performed every day over a period of 9 days and the obtained

chromatograms are shown in Figure 8 and Figure SI3. For the impregnated catalyst 25W/SBA, the monitoring of the chromatograms of the reaction medium showed significant conversion rate during 5 h of reaction but almost total deactivation at 24 h of test (Figure SI3). On 19WSBA, however, total conversion of Cx-BTs was observed for at least 6 days of run, a small quantity of unconverted species being only noticeable on the chromatograms after the 9th day (Figure 8).

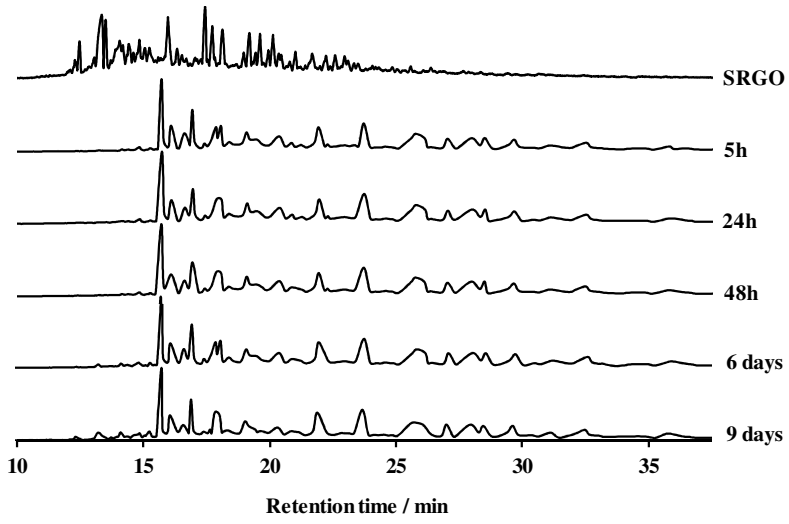

Figure 8: Chromatograms of the reaction mixture in the ODS of SGRO2000 on 19WSBA (fixed bed reactor, 75 °C, O/S = 25).

The lifetime of the incorporated catalyst is thus significantly longer than that of the impregnated one. Leaching of the active phase has been reported to be at the origin of deactivation in impregnated catalysts. Few studies have considered the ODS reaction in fixed bed reactors. Rapid deactivation of impregnated Mo/Al_2O_3 catalysts was observed by several authors and related to Mo leaching during reaction [21,50-52]. Cedeno *et al.* measured a decrease of conversion in the ODS of DBT from 47% to 10% in 20 hours of run, associated to 25% of Mo species leached out [52]. In the ODS of a Light Cycle Oil (LCO), Chica *et al.* observed 18% of Mo being leached out after 8 h of run [21]. In batch reactor, several authors have related the stability of direct synthesis HPW-silica based materials after several runs in ODS of DBT to a better resistance toward leaching. Li *et al.* have observed a decrease in sulfur removal by 2.1% and 8.3% after 4 runs on 20% HPW on HMS prepared by direct synthesis and wet impregnation respectively, with a corresponding decrease in the HPW content by 4.2% and 13.7% [30].

Similarly, TUD-1 type silica catalysts incorporated by HPW showed a low leaching of HPW species leading to a small decrease (2%) in the desulfurization rate after three cycles of catalysis [25].

In our study, significantly higher resistance towards deactivation of the incorporated catalyst was observed compared to impregnated one: indeed the synthesis route chosen allowed to develop interaction between the active phase and the support, which can minimize leaching, as evidenced by ToF-SIMS analysis. Moreover, this longer lifetime has been demonstrated in real conditions: in continuous ODS testing of a SRGO 2000 ppmS in a fixed bed reactor, and over a period of 9 days. The lower efficiency of incorporated catalysts compared to impregnated ones in ODS reaction carried out in a batch reactor is clearly compensated by their resistance towards leaching of the active phase in a continuous test, more representative of industrial conditions. It is thus of paramount importance to evaluate the catalysts performance in real conditions. Efficiency is indeed a key parameter, but more important is the necessity to optimize their life time in industrial conditions.

Conclusions

HPW-SBA based catalysts (xWSBA) were prepared by a direct synthesis method involving P123 and CTAB as structure directing agents and by incipient wetness impregnation for comparison purpose (xW/SBA). SBA textural properties were preserved upon incorporation and the HPW species were still present after calcination. The solids were first evaluated in batch reactor in the ODS of DBT (500 to 1500 ppmS) and of a SRGO 2000 ppmS. The xWSBA solids were found efficient, with, for the catalyst having the highest loading 19WSBA, 88% of DBT converted in the ODS of model feed and 100 % of Cx-BTs in 40 min in the ODS of real feed. Higher performance was obtained for the impregnated catalysts with, for 25W/SBA, 97% of DBT conversion and 100% of converted Cx-DBTs in 5 min. This difference in activity was attributed to a better accessibility of the active species present at the surface of the support in the case of impregnated solids whereas in the case of incorporated HPW, they are more embedded within the silica framework. However, in continuous performance evaluation in a fixed bed reactor, 19WSBA catalyst showed a stable conversion in the ODS of SRGO 2000 ppmS for almost 9 days, with only some unconverted Cx-BTs remaining, while in 24 h the impregnated solid 25W/SBA was almost completely deactivated. This resistance to deactivation of the 19WSBA solid was related to

the incorporation of HPW limiting its leaching during reaction. Interaction of HPW with the support was evidenced for the first time by ToF-SIMS analysis. In both impregnated and incorporated solids the emission of $Si_2WO_8H^-$ fragments was detected, with a quantity much higher, at similar HPW loading, for the incorporated solid than for the impregnated one. This study highlights the importance of evaluating ODS catalysts in realistic conditions, that is, in fixed bed reactor and in the presence of real feed. Indeed, if efficiency of the catalyst is a basic requirement in the implementation of any process, its resistance to deactivation is a key parameter to address for further developments especially in ODS reaction where leaching of the active phase is commonly reported.

Acknowledgements

Chevreul Institute (FR 2638), Ministère de l'Enseignement Supérieur et de la Recherche, Région Nord – Pas de Calais and FEDER are acknowledged for supporting and partially funding this work.

References

1. S. Wei, H. He, Y. Cheng, C. Yang, G. Zeng, L. Kang, H. Qian, C. Zhu, Fuel 200 (2017) 11-21. https://dx.doi.org/10.1016/j.fuel.2017.03.052

2. L. Kang, H. Liu, H. He, C. Yang, Fuel 234 (2018)1229-1237. https://doi.org/10.1016/j.fuel.2018.07.148.

3. S. Wei, H. He, Y. Chang, C. Yang, G. Zeng, L. Qiu, RSC Adv. 6 (2016) 103253-103269. http://dx.doi.org/10.1039/C6RA22358C

4. A. Ishihara, D. Wang, F. Dumeignil, H. Amano, E.W. Qian, T. Kabe, Appl. Catal. A Gen. 279 (2005) 279-287. https://doi.org/10.1016/j.apcata.2004.10.037

5. S. Otsuki, T. Nonaka, N. Takashima, W. Qian, A. Ishihara, T. Imai, T. Kabe, Energy Fuels 14 (2000) 1232-1239. https://doi.org/10.1021/ef000096i

6. T.C. Chen, J.F.F. Sapitan, F.C. Ballesteros Jr, M.C. Lu, J. Clean. Prod. 124 (2016) 378-382. https://doi.org/10.1016/j.jclepro.2016.03.004

7. A. Stanislaus, A. Marafi, M. S Rana, Catal. Today 153 (2010) 1-68. https://doi.org/10.1016/j.cattod.2010.05.011

8. M.A. Rezvani, A.F. Shojaie, M.H. Loghmani, Catal. Commun. 25 (2012) 36-40. https://doi.org/10.1016/j.catcom.2012.04.007

9. M. Li, M. Zhang, A. Wei, W. Zhu, S. Xun, Y. Li, H. Li, H. Li, J. Mol. Cat. A: Chem. 406 (2015) 23-30. https://dx.doi.org/10.1016/j.molcata.2015.05.007

10. S. Xun, W. Zhu, F. Zhu, Y. Chang, D. Zheng, Y. Qin, M. Zhang, W. Jiang, H. Li, Chem. Eng. J. 280 (2015) 256-264. https://doi.org/10.1016/j.cej.2015.05.092

11. H. Zheng, Z. Sun, X. Chen, Q. Zhao, X. Wang and Z. Jiang, Appl. Catal. A Gen. 467 (2013) 26-32. https://doi.org/10.1016/j.apcata.2013.06.026

12. W. Trakarnpruk, K. Rujiraworawut, Fuel Proc. Technol. 90 (2009) 411-414. https://doi.org/10.1016/j.fuproc.2008.11.002

13. A.E.S. Choi, S. Roces, N. Dugos, M.W. Wan, Sustain. Environ. Res. 26 (2016) 184-190. https://doi.org/10.1016/j.serj.2015.11.005

14. M. Te, C. Fairbridge, Z. Ring, Appl. Catal. A Gen. 219 (2001) 267-280. https://doi.org/10.1016/S0926-860X(01)00699-8

15. M.D.G. de Luna, M.W. Wan, L.R. Golosinda, C.M. Futalan, M.C. Lu, Energy Fuels 31 (2017) 9923-9929. https://doi.org/10.1021/acs.energyfuels.7b01773

16. G. Wang, Y. Han, F. Wang, Y. Chu, X. Chen, React. Kinet. Mech. Cat. 115 (2015) 679-690. https://doi.org/10.1007/s11144-015-0869-5

17. D. Wang, N. Liu, J. Zhang, X. Zhao, W. Zhang, M. Zhang, J. Mol. Catal. A Chem. 393 (2014) 47-55. https://doi.org/10.1016/j.molcata.2014.05.026

18. Z.E.A. Abdalla, B. Li, Chem. Eng. J. 200 (2012) 113-121. https://doi.org/10.1016/j.cej.2012.06.004

19. G. Estephane, C. Lancelot, P. Blanchard, J. Toufaily, T. Hamiye, C. Lamonier, RSC Adv. 8 (2018) 13714-13721. https://doi.org/10.1039/C8RA01542B

20. J. Yuan, J. Xiong, J. Wang, W. Ding, L. Yang, M. Zhang, W. Zhu, H. Li, J. Porous Mat. 23 (2016) 823-831. https://doi.org/10.1007/s10934-016-0137-8

21. A. Chica, A. Corma, , M. Dómine, J. Catal. 242 (2006) 299–308. https://doi.org/10.1016/j.jcat.2006.06.013

22. G. Luo, L. Kang, M. Zhu, B. Dai, Fuel Process. Technol. 118 (2014) 20-27.
https://doi.org/10.1016/j.fuproc.2013.08.00

23. D. Xie, Q. He, Y. Su, T. Wang, R. Xu, B. Hu, Chinese J. Catal. 36 (2015) 1205-1213.
https://doi.org/10.1016/S1872-2067(15)60897-X

24. X.N. Pham, D.L. Tran, T.D. Pham, Q.M. Nguyen, V. Thi Tran Thi, H.D. Van, Adv. Powder Technol. 29 (2018) 58-65. https://doi.org/10.1016/j.apt.2017.10.01

25. L. Tang, G. Luo, M. Zhu, L. Kang, B. Dai, J. Ind. Eng. Chem. 10 (2013) 620-626.
https://doi.org/10.1016/j.jiec.2012.09.015

26. B.C. Gagea, Y. Lorgouilloux, Y. Altintas, P.A. Jacobs, J.A. Martens, J. Catal. 265 (2009) 99-108.
https://doi.org/10.1016/j.jcat.2009.04.017

27. C. Shi, R. Wang, G. Zhu, S. Qiu, J. Long, Eur. J. Inorg. Chem. (2005) 4801-4807.
https://doi.org/10.1002/ejic.200500488

28. R. Zhang, C. Yang, J. Mater. Chem. 18 (2008) 2691-2703.
https://doi.org/10.1039/B800025E

29. V. Dufaud, F. Lefebvre, Materials 3 (2010) 682-703. https://doi.org/10.3390/ma3010682

30. B. Li, W. Ma, J. Liu, C. Han, S. Zuo, X. Li, Catal. Commun. 13 (2011) 101–105.
https://doi.org/10.1016/j.catcom.2011.07.009

31. X. Li, S. Huang, Q. Xu, Y. Yang, Transit. Metal Chem. 34 (2009) 943-947.
https://doi.org/10.1007/s11243-009-9285-x

32. J. Qiu, G. Wang, Y. Zhang, D. Zeng, Y. Cheng, Fuel 147 (2015) 195-202.
https://doi.org/10.1016/j.fuel.2015.01.064

33. Y. Du, P. Yang, S. Zhou, J. Li, X. Du, J. Lei, Mater. Res. Bull. 97 (2018) 42-48.
https://doi.org/10.1016/j.materresbull.2017.08.034

34. D. Shen, Y. Dai, J. Han, L. Gan, J. Liu, M. Long, Chem. Eng. J. 332 (2018) 563-571.
https://doi.org/10.1016/j.cej.2017.09.087

35. X-S Wang, L. Li, J. Liang, Y-B Huang, R. Cao, ChemCatChem 9 (2017) 971-979.
https://doi.org/10.1002/cctc.201601450

36. D. Zhao, Q. Huo, J. Feng, B.F. Chmelka, G.D. Stucky, J. Am. Chem. Soc. 120 (1998) 6024-6036. https://doi.org/10.1021/ja974025i

37. V. Dufaud, F. Lefebvre, G. P. Niccolai, M. Aouine, J. Mater. Chem. 19 (2009) 1142-1150. https://doi.org/10.1039/B816172K

38. M.A. Safa, T. Al-Shamary, R. Al-Majren, R. Bouresli, X. Ma, Energy Fuels 31 (2017) 7464-7470. https://doi.org/10.1021/acs.energyfuels.7b01272

39. M.T. Nguyen Dinh, P. Rajbhandari, C. Lancelot, P. Blanchard, C. Lamonier, M. Bonne, S. Royer, F. Dumeignil, E. Payen, ChemCatChem 6 (2014) 328-338. https://doi.org/10.1002/c ctc.201300521

40. J.C. Juan, J. Zhang, M.A. Yarmo, J. Mol. Catal. A Chem. 267 (2007) 265-271. https://doi.org/10.1016/j.molcata.2006.09.029

41. S. Silva, A. Chaumonnot, A. Bonduelle-Skrzypczak, F. Lefebvre, S. Loridant, V. Dufaud, ChemCatChem 2 (2014) 464-467. https://doi.org/10.1002/cctc.201300800.

42. W. Kuang, A. Rives, M. Fournier, R. Hubaut, Appl. Catal. A Gen. 250, 2 (2003) 221-229. https://doi.org/10.1016/S0926-860X(03)00239-4

43. B. B. Dong, B. B. Zhang, H. Y. Wu, S. D. Li, K. Zhang, X. C. Zheng, Micropor. Mesopor. Mat. 176 (2013) 186-193. https://doi.org/10.1016/j.micromeso.2013.03.051

44. D. Chlala, J.M. Giraudon, N. Nuns, C. Lancelot, R.N. Vannier, M. Labaki, J.F. Lamonier, Appl. Catal. B Env. 184 (2016) 87-95. https://doi.org/10.1016/j.apcatb.2015.11.020

45. A.M. Vandenbroucke, M.T. Nguyen Dinh, N. Nuns, J.M. Giraudon, N. De Geyter, C. Leys, J.F. Lamonier, R. Morent, Chem. Eng. J. 283 (2016) 668-675. https://doi.org/10.1016/j.cej.2015.07.089

46. L. Yang, Y. Qi, X. Yuan, J. Shen, J. Kim, J. Mol. Catal. A Chem. 229 (2005) 199-205. https://doi.org/10.1016/j.molcata.2004.11.024

47. Z. Long, C. Yang, G. Zeng, L. Peng, C. Dai, H. He, Fuel 130 (2014) 19-24. https://dx.doi.org/10.1016/j.fuel.2014.04.005

48. J. Palomeque-Santiago, R. Lopez-Medina, R. Oviedo-Roa, J. Navarrete-Bolanos, R. Mora-Vallejo, J. A. Montoya de la Fuentes, J. M. Martinez-Magadan, Applied Catal. B Environ. 236 (2018) 326-337. https://doi.org/10.1016/j.apcatb.2018.04.079

49. P. Polikarpova, A. Akopyan, A. Shigapova, A. Glotov, A. Anisimov, E. Karakhanov, Energy Fuels 32 (2018) 10898-10903. https://doi.org/10.1021/acs.energyfuels.8b02583

50. K.S. Cho, Y.K. Lee, Appl. Catal. B Environ. 147 (2014) 35-42. https://doi.org/10.1016/j.apcatb.2013.08.017

51. V.V.D.N. Prasad, K.E. Jeong, H.J. Chae, C.U. Kim, S.Y. Jeong, Catal. Commun. 9 (10) (2008) 1966-1969. https://doi.org/10.1016/j.catcom.2008.03.021

52. L. Cedeno-Caero, M.A. Alvarez-Amparan, React. Kinet. Mech. Cat. 113 (1) (2014) 115-131. https://doi.org/10.1007/s11144-014-0729-8